A Cluster-Based Model for Charging a Single-Depot Fleet of Electric Vehicles

K. Šepetanc, *Student Member*, *IEEE* and H. Pandžić, *Senior Member*, *IEEE*

***Abstract*—This paper presents an operating model of a station that charges a single-depot and homogeneous fleet of electric vehicles (EV) performing deliveries. Both the charging station and the fleet of EVs are owned by a single delivery company. The operating model, whose goal is to find the optimal EV battery charging schedule, is based on a clustering technique that keeps track of the number of EVs with a specific battery state of energy (SoE), while considering battery degradation, variable (dis)charging efficiency and nonlinear charging speed. The proposed operating model can be used both for the day-ahead scheduling and for the intraday model-predictive-control-based adjustments. Due to its relatively low capacity as compared to other market participants, the charging station is considered to be a price taker in both markets. The price uncertainty is considered using the robust uncertainty budget.**

The paper also evaluates inefficiency of a commonly used charging policy, i.e. the baseline model, where every delivery vehicle is charged to at least a predetermined SoE before its departure. The presented model is evaluated using multiple case studies and sensitivity analysis.

As opposed to the non-clustered baseline model, the proposed approach scales well for very large fleets. Our analysis confirms that the results of the baseline model depend on the preset SoE at departure, while the proposed model provides optimal solution without assumptions on the departing SoE.

***Index Terms*—Clustering, EV fleet, charging station, battery model.**

NOMENCLATURE

A. Sets and Indices

$\mathcal{N}$	Set of battery SoE clusters, indexed by n and m.
$\mathcal{T}$	Set of time steps, indexed by t and k; T stands for the last time interval, t^{now} is the current time interval in MPC and t^{long} refers to time intervals beyond T.
Ξ	Set of decision variables.

B. Parameters

C^{bat}	Net battery energy capacity (MWh).
$K_n^{\text{ch}}/K_n^{\text{dis}}$	Number of neighbouring clusters a battery from cluster n can charge/discharge into.
N^{ch}	Number of chargers at the charging station.
N^{clus}	Number of battery SoE clusters.
$N^{\min}$	Minimum vehicle SoE cluster at return.
$N_{t,k,n}^{\text{out}}$	Number of deliveries at time t, with trip duration k and minimum SoE cluster requirement n, where $n > N^{\min}$.
N_n^{init}	Initial number of vehicles at the station for current MPC optimization.
q_t^{DA}	Station's day-ahead (dis)charging values (MWh).
q_t^{MPC}	Station's historic intraday MPC (dis)charging decisions (MWh).
b_t^{MPC}	Station's historic intraday MPC battery degradation costs (€).
$X_{t,n}^{\text{MPC}}$	Number of incoming vehicles that were dispatched by a past MPC optimization and that are returning at t with battery SoE in cluster n.
δ	Battery degradation cost (€/MWh).
$\eta_{n,m}$	Battery efficiency when dis(charging) from cluster n into cluster m.
λ_t	Average energy price on day-ahead market at time t (€/MWh).
λ_t^{ID}	Average energy price on intraday market at time t (€/MWh).
$\Delta\lambda_t$	Maximum energy price deviation at time t (€/MWh).
Γ	Uncertainty budget for energy price deviation.

C. Variables

Integer variables

$n_{t,n,m}^{\text{aux}}$	Auxiliary variable for simulating each SoE cluster n (dis)charging into cluster m.
$n_{t,n}^{\text{bat}}$	Number of vehicles at the charging station with SoE belonging to cluster n, where $n_{0,n}^{\text{bat}}$ is the initial state of battery clusters.
$x_{t,n}^{\text{in}}$	Number of incoming vehicles at time period t with battery SoE belonging to cluster n, where $n \geq N^{\min}$.
$x_{t,k,n,m}^{\text{out}}$	Number of outgoing vehicles at time t with trip duration k that needed at least cluster n SoE and received cluster m SoE at departure, where $n \wedge m > N^{\min}$.

Continuous variables

b_t^{deg}	Hourly battery degradation costs when performing arbitrage (€).
q_t	Station (dis)charging quantity (MWh).
b_t	Share of maximum price deviation at time t.
z/ω_t	Dual variables associated with the robust subproblem's first and second constraint respectively.
y_t	Linearization variable that provides absolute value of variable q_t.

The authors are with the University of Zagreb Faculty of Electrical Engineering and Computing (e-mails: karlo.sepetanc@fer.hr; hrvoje.pandzic@fer.hr). Their work was funded in part by the Croatian Science Foundation through project ANIMATION (contract no. IP-2019-04-9164). Employment of Karlo Šepetanc is fully funded by the Croatian Science Foundation under programme DOK-2018-09.

I. Introduction and Paper Positioning

A. Motivation

Electric Vehicles (EVs) are becoming one of the main pillars of the transition toward the clean energy consumption [1]. An important aspect of this transition is displacement of the existing vehicle fleets of delivery companies and similar businesses with EVs [2]. Early-stage adoption of EVs in such companies is beneficial in two ways. First, delivery vehicles generally travel longer distances than personal vehicles, resulting in a greater climate impact. Second, they do not depend on the public charging infrastructure as they always start their trip from a central warehouse, which avoids the public fast-charging station deployment issue [3]. Therefore, only a single, although high-capacity, charging station is needed at the depot to cover the charging needs of an entire fleet. In this paper, the depot refers to one single location where all deliveries start and end. After each delivery, regardless how many actual locations it includes, the vehicles return to the station for charging and loading the delivery goods. The EVs are homogeneous, meaning they all have the same battery type, and they can only be charged at the depot charging station. This charging station contains multiple charges that impose a limit on the number of EVs that can be charged simultaneously.

An important aspect of the EV fleet scheduling is battery modeling. Since vast majority of EVs use lithium-ion-based batteries, we examine three pivotal specifics of the lithium-ion batteries, often ignored in the literature. The first one is battery degradation, which reduces the extent of exercising energy arbitrage, i.e. purchasing energy when the price is low in order to sell it later at a higher price. The market price difference to perform arbitrage now needs to be sufficient to cover for negative effects of the battery cycle efficiency and the battery degradation cost [4]. The second aspect is the battery's nonlinear charging curve. While the batteries can be discharged at the same rate irrespective of its state of energy (SoE), their charging ability reduces as the SoE increases. Ignoring this fact can result in charging schedules infeasible in reality, as demonstrated in [5]. The final significant modeling specific of lithium-ion batteries is their variable efficiency. Higher efficiency levels are achieved for slower (dis)charging processes, while battery charging at high power significantly reduces the cycle efficiency [6]. Efficiency of AC-DC converters used to (dis)charge batteries is neglected as it sits around 0.98–0.99% throughout the entire output power range [7]. In order to make the model proposed in this paper realistic, we consider all three of these battery modeling aspects in this paper.

Focus on the model's scalability and numerical tractability are often overshadowed by the researchers desire to capture high level of operation details. However, in this work we put focus on both the modeling details and the numerical tractability. To this end, in addition to the day-ahead scheduling, we leverage computational tractability of the presented method to implement an indraday model predictive control (MPC). The MPC reoptimizes the given day-ahead schedule at every time period considering the EV delivery uncertainty realizations and achieves results close to the results under perfect information.

B. Literature Review

Generally, the EV fleet charging issues can be categorized by the modeling approach and the type of programming to solve the model. Two common modeling approaches are to observe each vehicle individually or to combine all vehicles into a single aggregate battery. The common programming approaches are linear programming (LP), mixed integer linear program (MILP), quadratic programming (QP), dynamic programming (DP), and heuristics.

Both the LP and QP methods for individual EV modeling are proposed in [8]. The LP method ignores battery losses, while the computation time of the QP method does not scale well, e.g. for 50 EVs it is 819 times slower than LP. A study presented in [9] analyzes a single EV during a 24-h period with known trip profiles and nonlinear battery characteristics using DP. Paper [10] expands the idea of modeling each vehicle individually using DP, but has to use an approximate DP method to compute the model whose computation time scales exponentially with the number of discretized variables. The authors in [11] propose an LP charging framework for EV aggregators composed of multiple control levels. The aggregator interacts with the market and allocates set points to the EVs for participation in regulation market. The presented model includes dependence of maximum charging power on SoE. A dynamic program for optimal coordination of an EV fleet utilizing multiple charging stations is proposed in [12]. The proposed dynamic model outperforms the static one as it manages uncertainty and adapts to realization of uncertainty in real time without significant computational burden. A heuristic day-ahead scheduling of a fleet of EVs is proposed in [13]. The day-ahead decision-making procedure is formulated as a Markov decision process. In the first phase the aggregator decides how much electricity to purchase in the day-ahead market, while in the second phase this electricity is distributed among EVs. An exact MILP approach solved using two heuristic methods for both the EVs trip scheduling and the charging is proposed in [14]. It does so in two steps, the first one determining the optimal schedule and the other one optimal charging distribution. The MILP model is viable only for small and medium fleets and fails to provide solution for 120 EVs.

As opposed to individual EV models, aggregate battery models are less computationally expensive. A framework that utilizes the summation of energy and power boundaries of individual EVs to represent the fleet's aggregate energy and power boundaries is presented in [15]. This aggregate battery model divides EVs in groups based on their batteries' laxity and SoE to calculate the achievable vehicle-to-grid capacity. Aggregate battery model described in [16] addresses the maximum charging power and SoE of an aggregate battery dependency on the number of vehicles at the charging station. However, it can not account for already fully charged EVs at the station or nonlinear (dis)charging efficiency and speed due to lack of information on individual EVs. It also assumes that all EVs depart fully charged from the station.

Another way of making the EV fleet scheduling problem computationally tractable is by introducing clusters. This tech-

nique is used to track more features than the aggregate battery models and to easily scale the model to large fleet of vehicles. While the vehicles are indistinguishable withing the same SoE cluster, the model presented in [17] computes how many and from which SoE clusters the vehicles should perform specific tasks. A reduced model based on the state space method that describes aggregated EVs with different connecting states and various SoE states is proposed in [18]. The presented work realizes the state transition prediction and the regulation capacity estimation using the Markov state transition method, characterized by its computational efficiency. A stochastic hybrid model to represent a large population of heterogeneous appliances, including interruptable ones such as EV chargers, is presented in [19]. The presented procedure first determines the optimal energy market and ancillary service quantities and then performs real-time operations to manage the load using direct load scheduling. A dynamic programming model solved using multi-stage stochastic programming is developed in [20] for participation of a plug-in EV aggregator managing the charging process of the vehicles connected to the same distribution network feeder. The vehicles are divided into departure classes. The results indicate that the proposed method may significantly reduce daily electricity costs for plug-in EVs as compared to opportunity charging. A simple, yet efficient approach to EV charging is proposed in [21]. It schedules the EV charging process while considering temporary charging interruption as the only allowed action. It is implemented with clustering technique that only allows the SoE transitions to the next SoE cluster, thus does not allow for discharging nor variable charging rate. A control framework for the aggregate charging dynamics of plug-in EVs is developed in [22]. It assumes that system operator is able to deliver a universal control signal to all EVs in range from 0 to 1, thus uniformly setting their charging power. The mathematical novelty is in new differential equations for collective charging.

The presented literature review indicates that the models on EV aggregation generally ignore the battery charging nonlinearities and variable (dis)charging efficiencies. Such nonlinearities are captured using equivalent-circuit models that provide an equivalent representation of battery cells based on laboratory measurements or estimation techniques. However, implementation of such highly nonlinear elements in already computationally intensive models such as EV aggregation cannot be performed directly. Thus, linear (or at least mixed-integer linear) models of batteries' nonlinearities have been developed to more accurately capture the battery (dis)charging process. Models that effectively reduce battery charging power in the constant-voltage phase are presented in [23] and [5]. The case study and laboratory measurements presented in [5] demonstrate that ignoring the reduction of battery charging power at high SoE would result in infeasible operating schedules. Another major simplification of battery models in EV aggregation models is constant battery (dis)charging efficiency. However, battery efficiency largely decreases with (dis)charging current. A mixed-integer linear model that considers the (dis)charging current when determining the cycle efficiency is constructed in [24]. The presented results of the case study indicate that the profits from energy arbitrage are overestimated by 10% when variable battery cycling efficiency is neglected.

The advantage of computationally efficient scheduling models is that they can be recast as MPC models and solve optimization problems close to real time. Advantages and difficulties of MPC-based charging strategies have been explored in [25]. A binary-variable free EV charging problem is addressed in [26]. It relaxes the nonconex quadratic initial form using a semidefinite relaxation to enhance computational tractability. In cases when the relaxation is not exact, it uses non-smooth optimization algorithm to enforce the exact rank-one matrix constraint. Paper [27] compares a simple LP MPC and a maximum charging power strategy. The MPC-based model in [28] also uses a simple battery model and puts emphasis on the interaction between the charging station and the power distribution system. To our knowledge, there is no work that effectively combines the high battery modeling details, cooptimizing the EV charging station and delivery tasks management, while formulating the problem in a computationally tractable manner suitable for MPC implementation.

C. Paper Contribution and Structure

Considering the literature gaps, this paper models both the battery charging nonlinearity and variable battery efficiency when scheduling vehicle deliveries concurrently with the charging schedule. The uncertainty on the market prices is included in the model. The proposed framework easily scales for very large fleets of vehicles while the solution process guarantees optimality. Great computational tractability allows us to implement an intraday MPC model that reoptimizes the charging schedule due to delivery uncertainty realizations in real time. The model does not distinguish between individual EVs within the same SoE cluster, however it does compute how many and from which SoE clusters the EVs should perform the scheduled deliveries. The model is highly scalable since the number of variables does not depend on the number of EVs but only on the number of SoE clusters. The EV batteries are subject to three charging regimes: grid-to-battery (the most common one), battery-to-grid (when market prices are extremely high) and battery-to-battery (when market prices are extremely high and no EV batteries are sufficiently charged).

The contribution of the paper consists of the following:

1) Formulation of a computationally tractable optimal operating model of an EV depot charging station for delivery vehicles that minimizes electricity costs while implementing battery degradation, nonlinear (dis)charging efficiency and nonlinear charging speed. Due to high computational tractability, the model is also implemented in an MPC-based intraday framework with a purpose to adjust the day-ahead schedule upon the realization of uncertainty.
2) Evaluation of the proposed model by comparing it to the charging policy from the literature where every delivery vehicle has to be charged to at least some predetermined SoE to start a delivery and evaluation of the effect of the number of chargers at the station.

Rest of the paper is structured as follows. Section II introduces the proposed clustering technique and Section III

presents the mathematical formulation of both the day-ahead and intraday models. Case study Section IV consists of seven parts: input data description IV-A, and six case studies. The case studies assess the impact of the uncertainty budget on the objective function (Subsection IV-B), compare the proposed model to ad-hoc policies (Subsection IV-C), study the effect of the number of chargers at the station on feasibility and the objective function (Subsection IV-D), quantify the impact of battery degradation on exercising market arbitrage (Subsection IV-E), assess the effect of the battery capacity on the objective function value (Subsection IV-F) and study the efficiency of the proposed intraday MPC compared to a perfect-information model (Subsection IV-G). Computational tractability is discussed in Section V, while the final Section VI provides relevant conclusions.

II. Description of the Clustering Technique

In this paper we apply a clustering technique in which vehicles are clustered into predetermined SoE levels. The clusters are integer variables that support any number of vehicles without changing the number of constraints or variables in the model. The clustering structure is visualized in Fig. 1. In this simple example, there are only five SoE clusters (0%, 25%, 50%, 75% and 100%). The first and the last rows show the number of vehicles at the charging station at times $t-1$ and t, respectively, while the five rows in the middle show an auxiliary charging matrix. The auxiliary matrix has one row for each cluster. The first row of the auxiliary matrix indicates to which clusters did the empty batteries, i.e. the ones from the first cluster, from time period $t-1$ charge into. The second row indicates the same for the second cluster, and so on. The principle is explained in the following example. As displayed in the Fig. 1, there are two empty EVs at time $t-1$, one remains empty while the other one is charged to 25% (first row of the auxiliary matrix). Orange diagonal matrix elements represent the number of EVs that did not change their SoE, therefore numbers to the left of the diagonal elements indicate discharging and numbers to the right indicate charging. Thus, out of the two batteries at 50% SoE at t–1, one was discharged to 25% SoE, while the other one was charged to 75% SoE (third row of the auxiliary matrix). Clusters that are out of the (dis)charging range are grayed out and thus always equal to zero. In this sense, a variable (dis)charging speed is implemented. For example, the EVs with 50% SoE can be fully discharged, but can only be charged up to 75% SoE in a single time period (third row of the auxiliary matrix). From Fig. 1 one can notice that it requires at least three time intervals to fully charge an empty battery (cluster 1 $\rightarrow$ cluster 3 $\rightarrow$ cluster 4 $\rightarrow$ cluster 5). On the other hand, a fully charged battery can discharge completely in only two time steps (cluster 5 $\rightarrow$ cluster 3 $\rightarrow$ cluster 1). The number of EVs per cluster in the following time period corresponds to the vertical summation in the auxiliary charging matrix.

The advantage of the presented technique is in its ability to model high level of details of the battery characteristics. In the following example we demonstrate the necessity of the auxiliary matrix. Assume there are four EVs at the charging

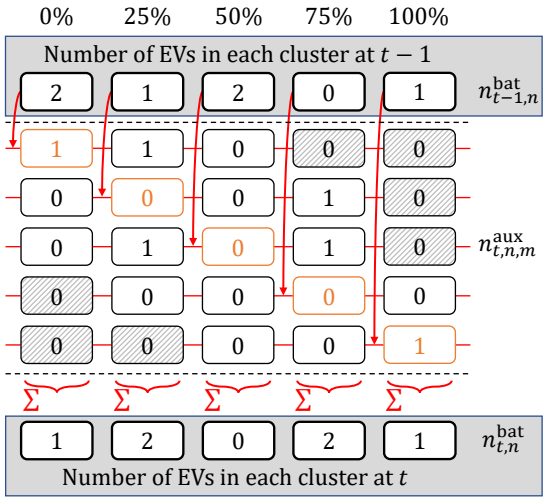

Fig. 1. Visualization of the clustered battery charging principle.

station and that two of them have their batteries charged to 50% and the other two to 75%. Also, assume that in the next time period at the charging station there is the same situation, two vehicles with 50% SoE and two with 75% and there were no incoming nor departing vehicles. The auxiliary matrix keeps track of the SoE transitions for each cluster individually, thus capturing if the 75% charged EVs discharged to 50% and the 50% charged EVs charged to 75% (this could actually happen in case of negative market prices) or no (dis)charging occurred at all. Despite the fact that the starting and final states of EVs at the station are the same, there are multiple combinations of SoE cluster transitions to achieve the resulting SoE state, each with different battery degradation and combined (dis)charging power. Keeping track of individual cluster SoE transitions enables implementation of battery degradation and variable battery efficiency.

Another important aspect of the proposed clustering technique is the interaction of the incoming and outgoing vehicles with the vehicles at the depot charging station. An example visualized in Fig. 2 shows six vehicles at the depot charging station (one with 0%, two with 25%, two with 75% and one with 100% SoE). The number of incoming vehicles is denoted in green (one with 0% and two with 25% SoE), and the vehicles departing to make deliveries are marked in red (one with 75% and one with 100% SoE). Generally, the incoming vehicles arrive with low SoE clusters, and departing ones leaved with high SoE clusters. The final number of EVs per cluster at the depot charging station is equal to the sum of the EVs at the station, the number of incoming vehicles and the negative of the number of departing EVs. On the example

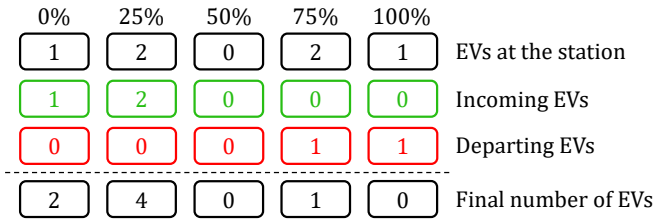

Fig. 2. Visualization of the vehicle exchange principle at the depot charging station.

in Fig. 2 the final number of EVs per cluster is shown in the last row.

The variable for the number of outgoing vehicles, $x^{\text{out}}_{t,k,n,m}$, has multiple indices since the model allows partially charged EVs to start a delivery if their SoE is sufficient to return to the depot. Namely, if an EV starts its delivery with the minimum required SoE for departure, it will return to the charging station with $N^{\min}$ SoE cluster. The $N^{\min}$ is a safety factor that address the uncertainty on the energy consumption during a trip. The trip schedules should be organised in a way to include the return SoE safety factor so that vehicles to not run out of energy during their trips. The SoE safety factory can be easily set to any value or even removed by setting $N^{\min}=1$ (cluster 1 represents 0% SoE). On the other hand, if EV starts the delivery with higher SoE, it will return with proportionally higher SoE level. This principle is depicted in Fig. 3. Assume the cluster resolution is 25% and $N^{\min}=2$ (25% SoE). If the delivery requires minimum SoE from cluster 3 (50% SoE) and a vehicle with SoE cluster 4 (75% SoE) performs the delivery, it will return with $N^{\min}+4-3=3$ SoE cluster or 50% SoE. In variable $x^{\text{out}}_{t,k,n,m}$ index t stands for departure time, index k stands for trip duration, index n stands for minimum required SoE and index m for the allocated vehicle's actual SoE. $x^{\text{out}}_{10,6,3,4}=3$ means there are 3 vehicles departing at time period 10 with trip duration of 6 time periods (1 hour and 30 minutes) on deliveries that require at least 50% SoE (third cluster) and vehicles have 75% SoE (fourth cluster), thus returning at the 16th time period with 50% SoE as described before. The uncertainties within this parameter include trip duration and required energy when finishing the trip. Both are addressed by using the expected worst-case values of these parameters.

III. Mathematical Model

In the following subsection we first present the day-ahead EV depot scheduling model in details and then present the characteristics of the intraday MPC-based model, which utilizes most of the constraints of the day-ahead model.

A. Day-ahead Model

The proposed model minimizes the total cost of purchasing electricity for a fleet of delivery EVs in the day-ahead market considering the degradation of EV batteries when discharging into the grid for arbitrage purposes (first line in eq. (1.1)). Time steps for calculation are set to 15-minute intervals to better capture (dis)charging nonlinearities and delivery durations. However, since the electricity markets mostly operate on one-hour resolution, the same price λ_t is used for all four 15-minute intervals. To implement this, we use the modulo operator, which returns the remainder after dividing one number by another, abbreviated as *mod*. If required, this can easily be updated to 15-minute markets. The objective function also contains a robust subproblem that addresses the uncertainty of the electricity price. The objective function of the robust subproblem (second line in eq. (1.1)) maximizes the damage that the price deviation $\Delta\lambda_t$ inflicts to the main objective function. The extent of the damage is controlled by auxiliary variable b_t, which takes values between 0 and 1 in each time period. For $b_t=1$, the maximum $\Delta\lambda_t$ price deviation occurs, either in positive or negative direction. The negative price deviation appears when the station is discharging, thus the absolute value operator flips the expression sign so that the robust problem inflicts damage to the main problem. The number of hours in which a price deviation occurs is defined by the user-controlled parameter Γ (third line in eq. (1.1)), which is usually referred to as the uncertainty budget. The higher the budget of uncertainty, the more damage is inflicted to the main objective function. Robust optimization framework was chosen over other risk metrics, e.g. conditional value-at-risk, as it does not increase the computational burden.

$$\begin{aligned}\underset{\Xi}{\text{Min}} \sum_{\substack{t\\ t \bmod 4=1}} \lambda_t\cdot(q_t+q_{t+1}+q_{t+2}+q_{t+3}) + \sum_t b^{\text{deg}}_t \\ +\underset{b_t}{\text{Max}}\{\sum_{\substack{t\\ t \bmod 4=1}} \Delta\lambda_t\cdot|q_t+q_{t+1}+q_{t+2}+q_{t+3}|\cdot b_t \\ \text{s.t.}\sum_{\substack{t\\ t \bmod 4=1}} b_t\le\Gamma,\ \ 0\le b_t\le 1\ \forall t: t \bmod 4=1\}\end{aligned} \tag{1.1}$$

subject to

$$n^{\text{bat}}_{t-1,n}-\sum_{\substack{k,m\\ m\le n\\ N^{\text{out}}_{t,k,m}>0}} x^{\text{out}}_{t,k,m,n}+\underset{n\ge N^{\min}}{x^{\text{in}}_{t,n}} = \sum_{m=n-K^{\text{dis}}_n}^{n+K^{\text{ch}}_n} n^{\text{aux}}_{t,n,m},\quad \forall t,n \tag{1.2}$$

$$n^{\text{bat}}_{t,n}=\sum_{\substack{m\\ m\ge n+K^{\text{dis}}_m\\ m\le n-K^{\text{ch}}_m}} n^{\text{aux}}_{t,m,n},\quad \forall t,n \tag{1.3}$$

$$\sum_{\substack{m\\ m\ge n}} x^{\text{out}}_{t,k,n,m}=N^{\text{out}}_{t,k,n},\quad \forall t,k,n: N^{\text{out}}_{t,k,n}>0 \tag{1.4}$$

$$x^{\text{in}}_{t,n}=\sum_{\substack{k,m\\ N^{\text{out}}_{t-k,k,m}>0}} x^{\text{out}}_{t-k,k,m,m+(n-N^{\min})},\quad \forall t,n: n\ge N^{\min} \tag{1.5}$$

$$\begin{aligned}\sum_n n^{\text{bat}}_{T,n}\cdot C^{\text{bat}}\cdot\frac{n-1}{N^{\text{clus}}-1}+\sum_{\substack{t,k,n,m\\ k>T-t\\ m\ge n\\ N^{\text{out}}_{t,k,n}>0}} x^{\text{out}}_{t,k,n,m}\cdot C^{\text{bat}}\cdot\frac{m-n+N^{\min}-1}{N^{\text{clus}}-1} \\ \ge\sum_n n^{\text{bat}}_{0,n}\cdot C^{\text{bat}}\cdot\frac{n-1}{N^{\text{clus}}-1}\end{aligned} \tag{1.6}$$

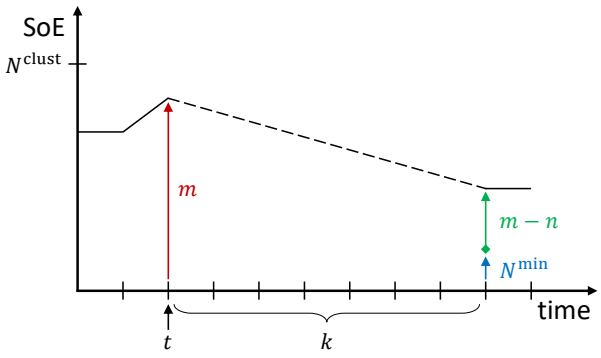

Fig. 3. Representation of a single vehicle with SoE cluster m going on a delivery at time t, with duration k, requiring minimum SoE cluster n.

$$b_t^{\text{deg}} = \sum_n \sum_{m=n-K_n^{\text{dis}}}^{n-1} \delta \cdot n_{t,n,m}^{\text{aux}} C^{\text{bat}} \cdot \frac{n-m}{N^{\text{clus}}-1}, \quad \forall t \quad (1.7)$$

$$q_t = \sum_n \left[\sum_{m=n-K_n^{\text{dis}}}^{n-1} n_{t,n,m}^{\text{aux}} \cdot C^{\text{bat}}/\eta_{n,m} \cdot \frac{m-n}{N^{\text{clus}}-1} - \sum_{m=n+1}^{n+K_n^{\text{ch}}} n_{t,n,m}^{\text{aux}} \cdot C^{\text{bat}} \cdot \eta_{n,m} \cdot \frac{n-m}{N^{\text{clus}}-1} \right], \quad \forall t \quad (1.8)$$

$$\sum_n \left[\sum_{m=n-K_n^{\text{dis}}}^{n-1} n_{t,n,m}^{\text{aux}} + \sum_{m=n+1}^{n+K_n^{\text{ch}}} n_{t,n,m}^{\text{aux}} \right] \leq N^{\text{ch}}, \quad \forall t \quad (1.9)$$

Constraint (1.2) distributes the EVs from each cluster into the auxiliary charging matrix $n_{t,n,m}^{\text{aux}}$ respecting the variable (dis)charging limits K_n^{ch} and K_n^{dis}. The number of vehicles that remain at the station is equal to the number vehicles that were located there in previous time period $n_{t-1,n}^{\text{bat}}$ increased for the number of incoming $x_{t,n}^{\text{in}}$ and decreased for the number of outgoing vehicles $x_{t,k,n,m}^{\text{out}}$. Number of outgoing vehicles $x_{t,k,n,m}^{\text{out}}$ is obviously a very sparse variable as it considers all possible departure times t, trip durations k, minimum vehicle SoE requirements n, and actual vehicle SoE level m. Thus, the outgoing vehicles variable sparsity is implemented using the summation and variable conditions, i.e. the condition that such delivery can exist $N_{t,k,n}^{\text{out}} > 0$ and condition that the assigned EVs have sufficient SoE $m \geq n$. Similarly, incoming vehicles are added to the constraint only for SoE's that satisfy minimum return SoE requirement $n \geq N^{\min}$.

Constraint (1.3) vertically sums the auxiliary charging matrix as displayed in Fig. 1. Conditions under a sum, $m \geq n + K_m^{\text{dis}}$ and $m \leq n - K_m^{\text{ch}}$, serve to prevent the summation of the values that are out of possible charging range so that, since those variables are always zero, are not sent to the solver.

Number of outgoing ($x_{t,k,n,m}^{\text{out}}$) and incoming ($x_{t,n}^{\text{in}}$) vehicles is modeled in constraints (1.4) and (1.5). Constraint (1.4) enforces the requirement that all deliveries ($N_{t,k,n}^{\text{out}}$) have to be served and the sum over m index, such that $m \geq n$, is there to allow any EV that satisfies delivery's minimum SoE requirement n to start the delivery. In the constraint (1.5), the vehicles that start deliveries at time $t-k$ that take k periods of time to complete (right side indices) will return at time t (left side index). Also, m charged vehicles that start deliveries with m minimum SoE, will return with $m = N^{\min}$ SoE. However, those that are charged higher at the start, will also return with proportionally higher SoE. The $(n - N^{\min})$ in the index $m + (n - N^{\min})$ stands for how much higher is the EVs starting SoE than the deliveries minimum. The sum collects all EVs with the same return characteristics, while the sum condition $N_{t-k,k,m}^{\text{out}} > 0$ prevents summation of variables that are always zero due to no deliveries.

Constraint (1.6) is the charging station energy preservation constraint. It requires that the total battery energy at the end of a simulated day (plus energy of vehicles that are returning after the midnight) is at least equal to the overall energy stored in the EVs' batteries at $t = 0$. The intent of this constraint is to prevent the so-called energy drainage, i.e. earnings due to discharging of the energy charged during the previous day, which would unjustly reduce the energy costs on the simulated day. SoE is calculated as a multiplication of the number of vehicles, net EV battery capacity and SoE share of a fully charged battery a given SoE cluster represents. The summation condition $k > T - t$ means that a delivery lasts longer than the end of a day while conditions $m \geq n$ and $N_{t,k,n}^{\text{out}}$ ensure $x_{t,k,n,m}^{\text{out}}$ sparsity by implying that outgoing vehicles have sufficient SoE for a delivery and that such deliveries exist.

Constraints (1.7) and (1.8) model battery degradation and net energy charged from the grid. Degradation is defined as a total negative SoE change for vehicles at the station, i.e. vehicles discharging into the power grid. In eq. (1.7), the battery degradation is proportional to the difference of the SoE cluster change $n-m$ when discharging a battery. Similarly, the energy discharged/charged from/into the battery is proportional to the difference of the SoE cluster change $m - n$. However, in constraint (1.8) the efficiency parameter $\eta_{n,m}$ is indexed to account for nonlinear (dis)charging efficiency when a battery changes its SoE from cluster n to cluster m.

Limitation on the number of chargers in the charging station is imposed in (1.9) as maximum number of SoE changes in the auxiliary charging matrix, i.e. sum of non-diagonal values in variable $n_{t,n,m}^{\text{aux}}$ (see Fig. 1).

Problem (1) cannot be directly solved because of the subproblem in (1.1) arising from the robust optimization approach. Therefore, objective function (1.1) needs to be rewritten to eliminate the robust subproblem using duality properties as explained in [29]. The resulting objective function and additional constraints are:

$$\underset{\Xi \cup \{z,\omega_t,y_t\}}{\text{Min}} \sum_{\substack{t \\ t \bmod 4 = 1}} \lambda_t \cdot (q_t + q_{t+1} + q_{t+2} + q_{t+3}) + \sum_t b_t^{\text{deg}} + z \cdot \Gamma + \sum_{\substack{t \\ t \bmod 4 = 1}} \omega_t \quad (2.1)$$

subject to

$$z + \omega_t \geq \Delta\lambda_t \cdot y_t, \quad \forall t : t \bmod 4 = 1 \quad (2.2)$$

$$-y_t \leq q_t + q_{t+1} + q_{t+2} + q_{t+3} \leq y_t, \quad \forall t : t \bmod 4 = 1 \quad (2.3)$$

$$z \geq 0 \quad (2.4)$$

$$\omega_t \geq 0, \quad \forall t : t \bmod 4 = 1 \quad (2.5)$$

The final MILP day-ahead model minimizes (2.1) over $\Xi \cup \{z, \omega_t, y_t\}$ subject to constraints (1.2)–(1.8) and (2.2)–(2.5), where $\Xi = \{n_{t,n,m}^{\text{aux}}, n_{t,n}^{\text{bat}}, x_{t,n}^{\text{in}}, x_{t,k,n,m}^{\text{out}}, b_t^{\text{deg}}, q_t\}$. Constraint (1.9) is only included in the model in case study IV-D for evaluating the effect of the number of chargers at the station.

B. MPC Model

In addition to the presented day-ahead model, we present its intraday MPC version. Objective function (3.1) minimizes electricity expenses in the indraday market, which consist of the previously purchased quantities[1] q_t^{MPC} and quantities to

[1]This parameter is not required in the objective function, but we include it so the objective function includes true daily costs instead of only from time period t^{now} onward.

be purchased in the coming time periods q_t. The objective function also includes the previous battery degradation cost parameter, b_t^{MPC}, and future battery degradation cost variable b_t^{deg}. The intraday market is on hourly basis, the same as the day-ahead market.

Most of the MPC constraints are analogous to the day-ahead model. The MPC counterparts of constraints (1.3), (1.4) and (1.7) only differ in the condition for which they repeat, $\forall t \geq t^{\mathrm{now}}$ instead of $\forall t$, i.e. they refer only to future time periods. Constraints (3.2), (3.5), (3.6) and (3.8) have more significant differences to their day-ahead counterparts (1.2), (1.5), (1.6) and (1.8), and they are thus fully stated below. Compared to (1.2), eq. (3.2) contains an additional parameter $X_{t,n}^{\mathrm{MPC}}$, which is the number of returning EVs at time t and SoE cluster n that were previously dispatched by the MPC to variable $x_{t,n}^{\mathrm{in}}$. Eq. (3.5) adds the $t-k$ condition to the sum on the right-hand side to prevent creation of $x_{t,k,n,m}^{\mathrm{out}}$ variable for the previous time periods. Energy neutrality constraint (3.6) as compared to eq. (1.6) includes an additional sum on the left-hand side containing parameter $X_{t^{\mathrm{long}},n}^{\mathrm{MPC}}$ to account for the energy in EVs scheduled for a delivery by a previous MPC run and returning after the end of the day. Thus, the parameter $X_{t^{\mathrm{long}},n}^{\mathrm{MPC}}$ is indexed using an extended set of time periods t^{long}. Constraint (3.8), as compared to eq. (1.8), adds a parameter of the day-ahead purchased energy $q_{t,n}^{\mathrm{DA}}$ to the energy purchased in the intraday market. Not that variable q_t always represents the energy purchased in the market, in model (1) this is day-ahead market and in model (3) this is intraday market.

$$\begin{aligned}\min_{\Xi} \; & \sum_{\substack{t \\ t \bmod 4 = 0 \\ t < t^{\mathrm{now}}}} \lambda_{t-3}^{\mathrm{ID}} \cdot (q_{t-3}^{\mathrm{MPC}} + q_{t-2}^{\mathrm{MPC}} + q_{t-1}^{\mathrm{MPC}} + q_t^{\mathrm{MPC}}) + \\ & \sum_{\substack{t \\ t \bmod 4 = 1 \\ t \geq t^{\mathrm{now}}}} \lambda_t^{\mathrm{ID}} \cdot (q_t + q_{t+1} + q_{t+2} + q_{t+3}) + \\ & \sum_{\substack{t \\ t \bmod 4 = 2 \\ t = t^{\mathrm{now}}}} \lambda_{t-1}^{\mathrm{ID}} \cdot (q_{t-1}^{\mathrm{MPC}} + q_t + q_{t+1} + q_{t+2}) \\ & \sum_{\substack{t \\ t \bmod 4 = 3 \\ t = t^{\mathrm{now}}}} \lambda_{t-2}^{\mathrm{ID}} \cdot (q_{t-2}^{\mathrm{MPC}} + q_{t-1}^{\mathrm{MPC}} + q_t + q_{t+1}) + \sum_{\substack{t \\ t < t^{\mathrm{now}}}} b_t^{\mathrm{MPC}} \\ & \sum_{\substack{t \\ t \bmod 4 = 0 \\ t = t^{\mathrm{now}}}} \lambda_{t-3}^{\mathrm{ID}} \cdot (q_{t-3}^{\mathrm{MPC}} + q_{t-2}^{\mathrm{MPC}} + q_{t-1}^{\mathrm{MPC}} + q_t) + \sum_{\substack{t \\ t \geq t^{\mathrm{now}}}} b_t^{\mathrm{deg}} \end{aligned} \tag{3.1}$$

subject to

$$\begin{aligned} & n_{t-1,n}^{\mathrm{bat}} + N_n^{\mathrm{init}} - \sum_{\substack{k,m \\ m \leq n \\ N_{t,k,m}^{\mathrm{out}} > 0}} x_{t,k,m,n}^{\mathrm{out}} + x_{t,n}^{\mathrm{in}} + X_{t,n}^{\mathrm{MPC}} \\ & \quad = \sum_{m=n-K_n^{\mathrm{dis}}}^{n+K_n^{\mathrm{ch}}} n_{t,n,m}^{\mathrm{aux}}, \quad \forall t \geq t^{\mathrm{now}}, n \end{aligned} \tag{3.2}$$

$$x_{t,n}^{\mathrm{in}} = \sum_{\substack{k,m \\ N_{t-k,k,m}^{\mathrm{out}} > 0 \\ t-k \geq t^{\mathrm{now}}}} x_{t-k,k,m,m+(n-N^{\mathrm{min}})}^{\mathrm{out}}, \quad \forall t \geq t^{\mathrm{now}}, n : n \geq N^{\mathrm{min}} \tag{3.5}$$

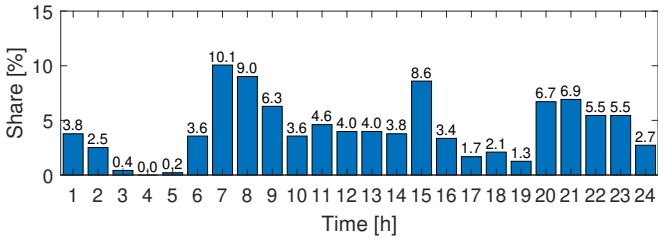

Fig. 4. Departure time distribution.

$$\begin{aligned} & \sum_n n_{T,n}^{\mathrm{bat}} \cdot C^{\mathrm{bat}} \cdot \frac{n-1}{N^{\mathrm{clus}}-1} + \sum_{\substack{t,k,n,m \\ k > T-t \\ m \geq n \\ N_{t,k,n}^{\mathrm{out}} > 0 \\ t \geq t^{\mathrm{now}}}} x_{t,k,n,m}^{\mathrm{out}} \cdot C^{\mathrm{bat}} \cdot \frac{m-n+N^{\mathrm{min}}-1}{N^{\mathrm{clus}}-1} \\ & + \sum_{\substack{t_n^{\mathrm{long}} \\ t^{\mathrm{long}} > T}} X_{t^{\mathrm{long}},n}^{\mathrm{MPC}} \cdot C^{\mathrm{bat}} \cdot \frac{n-1}{N^{\mathrm{clus}}-1} \geq \sum_n n_{0,n}^{\mathrm{bat}} \cdot C^{\mathrm{bat}} \cdot \frac{n-1}{N^{\mathrm{clus}}-1} \end{aligned} \tag{3.6}$$

$$\begin{aligned} q_t + q_t^{\mathrm{DA}} = \sum_n \Bigg[& \sum_{m=n-K_n^{\mathrm{dis}}}^{n-1} n_{t,n,m}^{\mathrm{aux}} \cdot C^{\mathrm{bat}} / \eta_{n,m} \cdot \frac{m-n}{N^{\mathrm{clus}}-1} \\ & - \sum_{m=n+1}^{n+K_n^{\mathrm{ch}}} n_{t,n,m}^{\mathrm{aux}} \cdot C^{\mathrm{bat}} \cdot \eta_{n,m} \cdot \frac{n-m}{N^{\mathrm{clus}}-1} \Bigg], \quad \forall t \geq t^{\mathrm{now}} \end{aligned} \tag{3.8}$$

MPC model minimizes (3.1) over the same Ξ as the day-ahead model, subject to constraints (3.2)–(3.8). Each iteration increases t^{now} to the next time period and updates the buffer parameters according to formulas: $X_{t^{\mathrm{long}},n}^{\mathrm{MPC}} = X_{t^{\mathrm{long}},n}^{\mathrm{MPC}} + \sum_{\substack{k,m \\ N_{t-k,k,m}^{\mathrm{out}} > 0 \\ t-k=t^{\mathrm{now}}}} x_{t-k,k,m,m+(n-N^{\mathrm{min}})}^{\mathrm{out}}$, $N_n^{\mathrm{init}} = n_{t^{\mathrm{now}},n}^{\mathrm{bat}}$ and $b_{t^{\mathrm{now}},n}^{\mathrm{MPC}} = b_{t^{\mathrm{now}},n}^{\mathrm{deg}}$.

IV. Case Study

A. Input Data

The case study presents the results of optimal operation of a charging station for an EV delivery fleet with 100 EVs and 487 scheduled deliveries during the simulated day. Statistical data on the departure times and travel distances, as well as average vehicle speed and standard deviations are obtained from [30]. EV departure time and delivery distance distributions for the observed day are shown in Figs. 4 and 5. While the average speed is 60 km/h, we assume 50 km/h for trips shorter than 100 km and 70 km/h for longer trips. Trip durations are derived using the assumed speeds and the available travel distance distribution with an additional 15 minutes for package handling at destination. Additional 30 minutes per trip are added to address uncertainty of the trip duration. This way, a conservative approach is employed to consider the worst-case realization of the uncertainty of the trip duration without introducing any additional variables or constraints. Complete data on the deliveries are stored in a single parameter, $N_{t,k,n}^{\mathrm{out}}$, where n denotes the SoE cluster needed for a vehicle to return with N^{min} SoE, which is set to five in this case study. Since there are 21 SoE clusters (5% each), cluster 5 corresponds to 20% SoE.

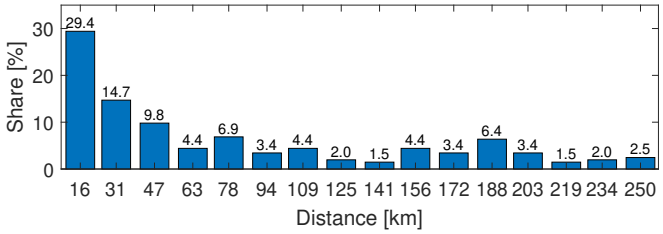

Fig. 5. Delivery distance distribution.

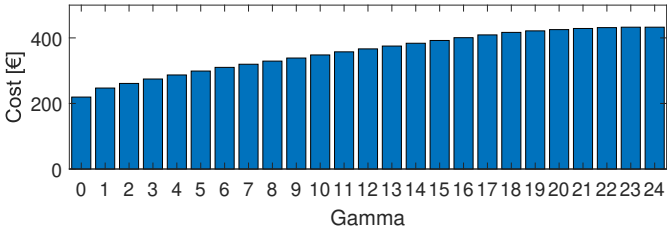

Fig. 6. Objective function value for different values of parameter Γ.

At the beginning of the optimization horizon, all EVs are located at the charging station. There are 47 fully charged EVs, i.e. they belong to cluster 21, and the remaining 53 have 20% SoE, i.e. they belong to cluster 5. The initial number of fully charged vehicles is about 1.5 times higher than the number of deliveries in the first 5 hours of the day to avoid potential initialization feasibility problems. EV batteries' maximum (dis)charging speed is 1C, i.e. at constant (dis)charging speed they would (dis)charge in 1 hour. However, this study encompasses a more advanced battery charging model presented in [5]. Batteries can charge in the constant current region at maximum rate of 1C (in this study we assume the constant current region from 0% to 55.7% SoE), while in the constant voltage region, from 55.7% SoE to 100% SoE, the maximum charging speed reduces linearly from 1C to 0C when full. Contrary to the charging speed, which reduces with SoE, maximum discharging rate is always 1C, which corresponds to actual lithium-based battery properties. Based on this, maximum charging speed in the model is calculated and rounded to the closest SoE cluster change per 15-minute interval. Consequently, it takes 1 hour and 45 minutes to fully charge an empty battery, although the nominal charging rate is 1C. Discharging, on the other hand, can be performed within 1 hour at 1C speed. Both the charging and discharging efficiencies are set to 0.9 at 1C and linearly increase to 0.9306 when (dis)charging at 0.2C [5]. Degradation costs are $\delta = 60$ €/MWh, which corresponds to the EV battery cost 300 €/kWh and 5,000 cycles over lifetime [31]. Battery energy capacity is $C^{\text{bat}} = 0.044$ MWh, which enables delivery routes up to 250 km.

Expected day-ahead electricity prices are average values during all Mondays in 2018 in the Denmark West bidding area [32]. Maximum energy price deviation δ_t is equal to the absolute value of annual maximum price variation from the average value. Intraday market prices are taken for Monday, 12 February 2018. Both the day-ahead and the intraday markets are hourly-based.

B. Impact of the Uncertainty Budget on the Objective Function

We analyze the results for uncertainty budget Γ ranging from 0, denoting the most most optimistic case when all prices are equal to their average values, to 24, which denotes the most conservative case when all prices are at the upper bound when buying and at the lower bound when selling energy. Parameter Γ is thus used to control the conservativeness of the solution. Fig. 6 shows the objective function values for different values of parameter Γ. The most optimistic setting for $\Gamma = 0$ results in €219,50 total electricity cost, while the most conservative solution results in almost double the cost, €432,69. However, already at $\Gamma = 18$ the objective function value becomes saturated and the overall cost does not increase much when further increasing Γ.

The importance of choosing an appropriate budget of uncertainty Γ is demonstrated in Fig. 7, which shows that different values of Γ result in severely different energy purchasing patterns. For $\Gamma = 0$, the charging station purchases energy for daily operation of its EVs in hour 4 and to reach the total EVs' SoE at the end of the day at least equal to the overall available energy at the beginning of the day in hour 24. Already for $\Gamma = 1$ the charging pattern is significantly different. This is because if the charging station purchases large quantities in a low-price hour, the robust subproblem increases the price in that specific hour to exacerbate the objective function the most. Since the cost minimization problem and the robust subproblem act in a coordinated way, the charging station schedules relatively low purchase quantities over multiple hours. For medium values of Γ (8, 12 and 16), the purchasing quantities are flat over the course of the day to minimize the damage the robust subproblem inflicts to the objective function. On the other hand, for high values of Γ the purchasing quantities are again grouped in the low-price periods. This is because the robust subproblem increases the prices in majority of hours and the main problem has no other options but to take the higher energy prices in most of the time periods. In other words, the assumed prices are at the upper price bound in Fig. 7.

It is worth noting that all the purchased energy quantities in Fig. 7 are positive, which means there is no EV discharging into the grid. This is a direct result of a relatively low price spread as compared to battery degradation effects and a high number of deliveries with respect to the fleet size (this is further elaborated in Sections IV.E and IV.F).

C. Comparison of the Proposed Model to Ad-hoc Policies

In order to quantify the benefits of the proposed model, we compare it to an ad-hoc policy proposed in [16], where it is assumed the EVs should leave the charging station fully charged. We perform this comparison using two indicators:

- objective function value;
- minimum number of EVs to perform the required deliveries.

Table I shows the objective function values and the minimum number of vehicles required to perform all deliveries for different minimum SoE policies for $\Gamma = 8$. The last row

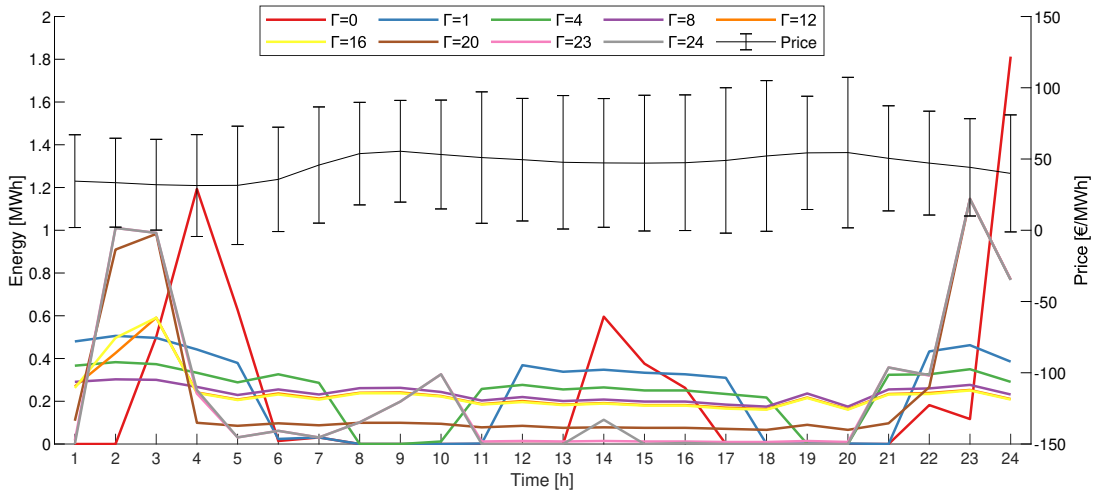

Fig. 7. Purchased energy quantities for different values of Γ; energy market price ranges.

shows the results of the model proposed in this paper, which does not have a minimum SoE at departure policy, instead it is a result of the optimization procedure. Requiring 100% SoE at departure results in 3.3% higher objective function value than what is achieved by our model. This is because the EV batteries are charged longer due to decreased charging speeds at high SoE. As a result, a part of the charged energy is purchased during the less favorable time periods in order to achieve 100% SoE at departure for deliveries where this is unnecessary.

The last column in Table I shows the minimum number of EVs required to perform all the deliveries. The initial number of vehicles per cluster is proportionally scaled. In the model itself, the minimum SoE policy is implemented by fixing variables $x^{\text{out}}_{t,k,n,m}$ with insufficient SoE cluster for the policy to 0. The number of required delivery vehicles is 26% higher for the 100% SoE policy as compared to the proposed model, which indicates that an inappropriate policy results in much higher investment costs. Reducing the minimum SoE to 80% is practically equivalent to the proposed model as 53% to 78% of all EVs in our model, depending on Γ, depart with SoE higher than 80%. Reducing policy's SoE requirement below 80% has no impact on the minimum number of vehicles nor the charging station's total costs.

Table II provides decisions taken by the charging station for the proposed model. The first line in each row shows the number of EVs at the station at the end of each hour, while the second line shows how many incoming and outgoing vehicles interacted with each SoE cluster. Entries with zero values are left blank. At the end of hour 1, 50 out of 53 EVs with SoE 20% charged to 35%, two charged to 30% and one charged to 25%. On the other hand, 19 out of 28 fully charged EVs went out to perform a delivery. During hour 2, the 53 EVs with low SoE further charged, resulting in 23 EVs with 55% SoE, 28 EVs with 45% SoE, one EV with 30% SoE, and one EV that departed with 35% during this hour (this EV returned during hour 3 with 20% SoE). Out of 19 EVs that went for a delivery during hour 1, 11 returned during hour 2, two of them with 85% SoE, three with 90% SoE and 6 with 95% SoE. The three EVs that departed with 95% SoE during hour 2 are among the ones that returned to the station earlier in the same hour. As a matter of fact, since the second hour was concluded without any EVs with 95% SoE, out of six EVs that arrived with this SoE, three were charged to 100% SoE and three departed for another delivery. This fast dynamics of EV charging and deliveries indicates the importance of higher EV charging resolution than one hour, which is the electricity market resolution. At the end of hour 7, all EVs were either performing a delivery or being charged to at least 90%. This shows that the charging station was getting prepared for the high number of deliveries during the morning and early afternoon. The proposed model uses EVs with low SoE to perform short deliveries, which is evident in hour 11, where one vehicle departs with 25% SoE and returns the next hour with 20% SoE. The SoE clusters in the second part of the day are relatively evenly distributed with relatively high number of EVs being fully charged in order to perform longer deliveries.

TABLE I
MINIMUM NUMBER OF EVS IN A FLEET FOR DIFFERENT POLICIES OF SOE AT DEPARTURE (ALL SIMULATIONS ASSUME $\Gamma = 8$).

Policy SoE	Objective function [€]	Min. number of EVs
100%	340.75	112
95%	331.58	97
90%	329.69	92
85%	329.59	91
80%	329.72	89
Proposed model	329.61	89

D. Effect of the Number of Chargers at the Station on Feasibility and Objective Function

The number of chargers at the charging station limits the number of vehicles that can be simultaneously charged and thus affects the model feasibility in two ways. First, with insufficient number of chargers, the station may not be able to satisfy the daily energy neutrality constraint (1.6) regardless of the number of EVs at the station, and second, it may not

TABLE II
EVs SoE CLUSTERS (ASSUMING 100 EVs AND $\Gamma = 8$).

	$n^{\mathrm{bat}}_{t,n}$ $(x^{\mathrm{in}}_{t,n}, \sum_{k,n} x^{\mathrm{out}}_{t,k,n,m})$																				
SoE / Hour	0%	5%	10%	15%	20%	25%	30%	35%	40%	45%	50%	55%	60%	65%	70%	75%	80%	85%	90%	95%	100%
0					**53**																**47**
1						**1** (0,0)	**2** (0,0)	**50** (0,0)													**28** (0,19)
2							**1** (0,0)	**0** (0,1)		**28** (0,0)		**23** (0,0)						**0** (2,0)	**2** (3,0)	**0** (6,3)	**26** (0,8)
3					**0** (1,0)	**1** (0,0)	**0** (0,1)					**28** (0,0)		**0** (1,0)	**6** (1,0)	**19** (1,0)	**2** (1,0)		**0** (2,0)	**0** (4,0)	**34** (0,0)
4						**0** (1,0)		**0** (1,0)	**4** (1,0)	**0** (1,0)	**0** (1,0)	**1** (0,0)	**11** (0,0)	**0** (1,0)	**19** (1,0)	**7** (1,0)		**14** (0,0)		**8** (0,0)	**34** (0,0)
5									**0** (1,0)	**0** (1,0)	**1** (0,0)		**5** (0,0)		**1** (0,0)	**11** (0,0)	**14** (0,0)	**26** (0,0)			**42** (0,0)
6																**1** (0,0)	**6** (0,0)	**13** (0,5)	**12** (0,0)		**50** (0,13)
7																	**0** (5,0)	**0** (2,0)	**2** (3,0)		**40** (0,50)
8														**1** (1,0)	**1** (1,0)	**1** (1,0)	**0** (1,1)	**5** (5,0)	**7** (7,2)	**0** (15,15)	**11** (0,29)
9								**1** (1,0)	**1** (1,0)	**1** (1,0)	**1** (1,0)	**1** (1,0)	**1** (1,0)	**2** (2,1)	**3** (3,1)	**4** (4,1)	**0** (2,2)	**10** (9,4)	**0** (6,13)	**0** (7,7)	**10** (0,1)
10								**2** (2,1)	**1** (3,1)	**5** (2,0)	**1** (3,1)	**4** (1,0)	**0** (1,2)	**2** (2,2)	**5** (5,3)	**8** (5,1)	**3** (3,0)	**16** (9,3)	**0** (1,1)		**7** (0,3)
11					**0** (1,0)	**0** (1,1)	**0** (2,0)	**1** (2,0)	**2** (3,1)	**0** (3,5)	**10** (4,1)	**4** (2,0)	**6** (7,0)	**2** (0,2)	**1** (1,1)	**4** (0,1)	**0** (0,1)	**5** (0,2)	**23** (0,0)	**0** (2,2)	**2** (0,5)
12					**5** (7,0)	**0** (1,0)	**3** (3,0)		**2** (5,0)		**1** (3,0)	**21** (0,0)	**0** (1,6)	**0** (0,1)	**5** (0,1)	**1** (0,2)	**1** (1,1)	**1** (0,5)	**0** (3,1)	**3** (0,0)	**22** (0,2)
13					**2** (6,0)		**0** (0,3)	**8** (0,0)	**1** (2,3)	**1** (0,0)	**0** (2,0)	**1** (6,0)	**2** (0,0)	**26** (0,0)	**1** (3,1)	**4** (3,1)	**0** (0,1)	**6** (0,1)		**0** (0,3)	**16** (0,6)
14					**0** (6,0)	**8** (0,0)		**1** (3,1)	**0** (0,1)	**8** (0,1)	**1** (1,0)	**0** (0,1)	**1** (1,2)	**1** (1,1)	**0** (0,1)	**20** (0,2)	**3** (1,1)	**5** (2,1)	**2** (0,0)	**0** (4,4)	**18** (0,3)
15					**0** (6,0)	**4** (0,8)	**2** (1,1)			**1** (0,0)	**0** (1,1)	**1** (2,0)	**9** (1,1)	**0** (1,1)	**1** (2,1)	**2** (0,1)	**2** (0,2)	**3** (2,5)	**18** (4,4)		**2** (0,18)
16					**0** (16,0)	**1** (0,4)	**15** (0,0)			**0** (0,1)	**2** (0,0)	**0** (0,1)	**0** (0,1)	**0** (1,0)	**13** (6,1)	**1** (0,2)	**0** (0,2)	**1** (0,3)	**0** (3,0)	**0** (5,2)	**26** (0,0)
17					**1** (11,0)	**2** (0,0)	**9** (0,1)	**0** (1,0)			**15** (0,2)			**4** (7,1)	**2** (0,1)	**12** (2,0)	**1** (2,0)	**4** (0,1)			**26** (0,0)
18					**0** (5,0)	**6** (0,0)	**2** (0,0)		**0** (4,0)	**16** (3,0)	**0** (2,0)	**2** (1,0)	**3** (0,0)	**17** (0,0)	**0** (0,1)	**1** (0,5)	**7** (0,1)	**3** (0,0)		**1** (0,0)	**25** (0,1)
19					**4** (4,0)	**7** (1,0)	**0** (0,2)	**1** (1,0)	**1** (1,0)	**16** (1,1)		**2** (0,0)	**3** (0,0)	**19** (2,0)	**3** (3,0)	**1** (0,0)	**7** (0,0)	**4** (1,0)		**1** (0,0)	**24** (0,1)
20					**4** (0,0)	**10** (3,0)	**1** (1,0)	**1** (0,0)	**0** (0,1)	**9** (1,8)		**1** (0,1)	**0** (0,3)	**19** (0,0)	**0** (0,3)	**0** (0,1)	**1** (0,6)	**1** (0,3)	**1** (1,0)	**0** (0,1)	**20** (0,4)
21					**0** (1,0)	**1** (0,10)		**1** (5,0)	**3** (3,0)	**0** (3,0)	**10** (1,1)	**7** (0,0)	**5** (0,0)	**0** (0,1)		**1** (6,6)	**12** (0,1)	**6** (0,1)	**0** (0,1)		**5** (0,15)
22					**0** (11,0)		**0** (1,0)		**13** (1,3)	**1** (0,0)	**1** (0,1)	**1** (0,1)	**1** (3,5)	**7** (5,0)	**9** (0,0)	**0** (0,1)	**5** (0,6)	**1** (3,6)	**2** (0,0)	**4** (0,0)	**2** (0,5)
23					**0** (5,0)	**3** (0,0)		**1** (2,0)	**1** (3,1)	**0** (0,1)	**5** (4,1)	**0** (0,1)	**12** (0,1)	**4** (5,0)	**3** (0,9)	**0** (5,3)	**9** (5,2)	**2** (0,1)	**0** (0,2)	**1** (0,4)	**7** (0,2)
24					**2** (7,0)	**0** (1,0)	**9** (0,0)	**0** (0,1)	**2** (2,1)		**0** (2,0)		**9** (2,0)	**0** (10,0)			**43** (5,0)	**0** (0,2)		**0** (0,1)	**0** (0,7)

be able to adequately charge enough EVs for the deliveries during peak hours. Infeasibilities due to peak-hour demand can be avoided by increasing the number of fully charged EVs initially located at the station. With only four chargers at the station, the model is always infeasible, with five it requires at least 187 EVs to perform the deliveries and with six chargers the minimum number of EVs is 89, which is the same as in Section IV-C where no limit on the number of chargers is imposed. However, when the 100% SoE policy is imposed, at least 9 chargers and 455 EVs or 10 chargers and 378 EVs are required to make all the deliveries. The minimum required number of EVs 112 is achieved with 16 chargers. Further increase in the number of chargers does not reduce the minimum required fleet size.

Number of chargers also affects the charging schedule. In the deterministic case, i.e. $\Gamma = 0$, the station tries to exploit the low-price periods and charge as many EVs as possible. Similar behavior is observed for very high uncertainty budget values where the price is effectively at the upper bound of the price span, thus regaining deterministic features. For intermediate Γ values, the charging schedule is spread more evenly across the day, making it less dependant on the number of chargers. The described behavior is visualized in Fig. 8. For $\Gamma = 0$, the station saves 14.4% or €37.23 on charging costs with 50 chargers as compared to only 6 of them. For $\Gamma = 24$ the savings are 11.8% or €57.89. The lowest 4.0% or €13.05

savings are observed for $\Gamma = 6$. Increasing the number of charges above 50 only negligibly further reduces the objective function value.

As compared to our model, when the 100% SoE is imposed the spread in the objective function between the high and the low number of chargers is significantly lower, as depicted in Fig. 9. The low spread occurs because the minimum number of chargers is 16, which is much higher than 6 chargers in the proposed model. Since the minimum number of 16 chargers is already quite high, the objective function does not reduce much for the increased number of chargers.

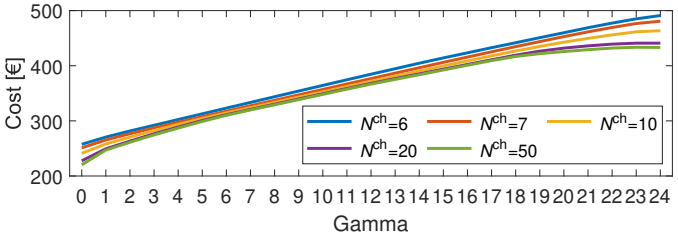

Fig. 8. Objective function values for different number of chargers and various Γ values (assuming 100 EVs).

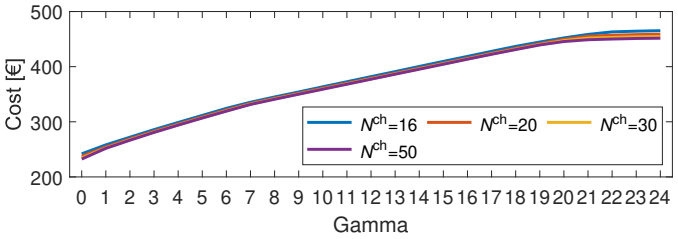

Fig. 9. Objective function values for different number of chargers and various Γ values when the 100% SoE at departure policy is imposed (assuming 112 EVs).

E. Effect of Battery Degradation on Objective Function

We assess the impact of the degradation cost by halving the value of parameter δ to €30/MWh and setting it to zero. The objective function values and overall energy discharged from all batteries are shown in Table III for $\Gamma = 0$. The results indicate that battery discharging to exercise market arbitrage is not very attractive even at zero degradation costs. This is a result of two factors. First, the price curve is relatively flat, i.e. there are no huge price spikes. Such price spread is far from being sufficient to cover for the €60/MWh or €30/MWh degradation costs. On top of that, the battery charging/discharging cycle is less than 100% efficient, which additionally discourages economic arbitrage. Second, the size of the fleet and the number of deliveries do not leave much opportunity to perform arbitrage as there is not much free battery capacity to be used for arbitrage purposes. To support this claim, we ran our model with no deliveries, unleashing the entire battery fleet capacity for arbitrage. The resulting objective function is -49€, achieved by discharging 4.4 MWh, indicating that each EV performs one charge-discharge cycle throughout the day.

The discharged quantities for higher values of Γ will always be lower as the robust formulation would cause additional damage to the objective function value.

F. Effect of Battery Capacity on Objective Function

In this case study we double the EV battery capacity as compared to the reference value from Section IV-A without altering the number of deliveries. This called also for doubling the SoE cluster resolution to 2.5% (41 clusters). The results from Table IV indicate 28.82 € (13.1%) savings by using larger batteries under the deterministic scenario ($\Gamma = 0$), but almost no difference under the robust case with $\Gamma = 8$. The advantage of larger batteries lies in their ability to charge faster in absolute terms since the same (dis)charging rate 1C is considered. In the deterministic case the charging station aggressively charges EVs in only few hours. The smaller batteries also need more energy to be charged since they are charged at higher rate than the bigger ones, thus reducing the charging efficiency. For $\Gamma = 8$ the station charges the EVs more evenly during the day, thus the difference between the larger and smaller batteries vanishes.

G. Intraday MPC

The obtained day-ahead schedule assumes the worst-case delivery times and energy consumptions, providing an extremely high feasibility level of the station's operation. However, such schedule leaves additional opportunities to reduce electricity costs during actual trip realisations, i.e. trips durations and EVs' consumptions during deliveries. Thus we conduct an MPC analysis that reschedules the deliveries and the charging schedule exploiting the intraday market and more accurate information on the current state of the batteries at the depot. The MPC model still anticipates the worst-case delivery and re-optimizes the charging schedule until the end of the day. This way the delivery schedule remains feasible, but the delivery station (depot) utilizes the updated information on the actual EVs' return times and SoE at retrieval.

The base case for this analysis assumes realization of the worst-case delivery characteristics. The Early case assumes that all EVs return 45 minutes earlier than predicted, the

TABLE III
IMPACT OF THE BATTERY DEGRADATION COST ON THE OBJECTIVE FUNCTION (ASSUMING $\Gamma = 0$ AND 100 EVS).

δ [€/MWh]	Objective function [€]	Total discharging [MWh]
60	219.50	0
30	219.50	0
0	218.02	0.473

TABLE IV
IMPACT OF THE BATTERY CAPACITY ON THE OBJECTIVE FUNCTION VALUE AND TOTAL CHARGED ENERGY FOR $\Gamma = 0$ AND $\Gamma = 8$.

Battery capacity [MWh]	Γ	Objective function [€]	Total charging [MWh]
0.044	0	219.50	5.712
0.088	0	190.68	5.688
0.044	8	329.20	5.669
0.088	8	329.04	5.667

Higher SoE case assumes all EV's return with 5% higher SoE than predicted, while in Early and higher SoE case the vehicles both return 45 minutes earlier and with 5% higher SoE. We also compare the results of the MPC calculation with the perfect information model, i.e. which up-front knows the correct delivery durations and consumptions. The perfect information cases are implemented by changing the delivery parameter $N^{\text{out}}_{t,n,m}$, while the MPC model by changing the number of returning vehicles in the following time period due to past dispatches $X^{\text{MPC}}_{t,n}$.

The results of the MPC model run for the day-ahead conservativeness parameter $\Gamma = 8$ and $\Gamma = 0$ are displayed in Tables V and VI. Base case, which assumes all vehicles return according the the conservative day-ahead plan, achieves savings in the intraday market despite the same realization of uncertainty compared to the day-ahead assumptions (higher negative number in Tables V and VI indicates greater savings). This is a result of different day-ahead and intraday market prices, which enable the depot to perform arbitrage between the day-ahead and intraday markets. Savings are higher for $\Gamma = 8$ because the depot purchases electricity more evenly throughout the day then for $\Gamma = 0$, where electricity is purchased only during nine hours (compare the corresponding curves in Figure 7). Having purchased energy in the day-ahead level allows selling energy in the intraday market without any actual EV discharging and thus avoiding the degradation costs and providing greater flexibility in the intraday trading regime. The MPC results present significant savings compared as compared to the day-ahead cost. For $\Gamma = 8$ the day-ahead charging costs are €329.20 and the intraday savings are €26.85, which is over 8%. Results for the Base case are the same when having perfect information and for MPC because the realizations of uncertainty are identical to the assumed worst-case realizations considered when deriving both the day-ahead and intraday schedules.

When EVs return earlier, i.e. for the Early case and $\Gamma = 8$, the MPC results in €27.89 savings, only slightly higher than in the Base case. Even when having the perfect information on the EV, the attained savings are only slightly higher. The overall savings are reduced by app. 50% when the day-ahead schedule is based on $\Gamma = 0$.

The Higher SoE case enables much higher savings as compared to the Early case, as the EVs actually consume less energy than anticipated. The savings for $\Gamma = 8$ are €55.81, again not much worse than when having a perfect information, which results in savings €58.22. For this case, the savings when using $\Gamma = 0$ at the day-ahead stage are not much lower than when using $\Gamma = 8$ (€55.81 compared to €41.78).

TABLE V
MPC RESULTS FOR RUNNING THE DAY-AHEAD MODEL WITH $\Gamma = 8$

Information	Case	Objective function [€]
Perfect	Base	-26.58
	Early	-28.06
	Higher SoE	-58.22
	Early and higher SoE	-58.85
MPC	Base	-26.58
	Early	-27.89
	Higher SoE	-55.81
	Early and higher SoE	-57.63

TABLE VI
MPC RESULTS FOR RUNNING THE DAY-AHEAD MODEL WITH $\Gamma = 0$

Information	Case	Objective function [€]
Perfect	Base	-12.56
	Early	-14.03
	Higher SoE	-44.20
	Early and higher SoE	-44.83
MPC	Base	-12.56
	Early	-13.87
	Higher SoE	-41.78
	Early and higher SoE	-43.61

Finally, the Early and higher SoE case results in the highest savings, but only slightly higher than the savings achieved under the Higher SoE case an much lower than the sum of the savings achieved by only the Early and the Higher SoE cases. This indicates that majority of the savings achieved by the Early and the Higher SoE cases overlap. Also, the utilization of the proposed MPC framework enables cost-savings very close to the ones that could be achieved by having a perfect information on the uncertain parameters.

V. Computational Tractability

The presented day-ahead and intraday models are computationally efficient and easy to solve despite the large number of integer variables. High efficiency is the result of a favorable integer variable relaxation that a solver performs internally at every solve procedure iteration. The relaxed variables have very close or exactly the same solution as the actual discrete model and thereby favourably guide the solver's branch and bound algorithm [17]. Share of integer variables that take integer values during the initial solver's relaxation is very large and displayed in Table VII. Additionally, when $\Gamma = 0$, the model can be computed within a few seconds to full optimality, i.e. no gap, and relaxed and discrete optimal values of the objective function are exactly the same. For other Γ values, the computations quickly reach 0.06% gap, but the full optimality is not achievable. The presented case study is solved to 0.1% gap using Gurobi 8.1.1 solver run by GAMS 28.2 on Intel desktop processor i5 7600 (4x3.9GHz) and is available for download at the link [33]. For the day-ahead optimization, the average computation time was 6 seconds and no computation lasted longer than 10 seconds. The longest MPC run, which consists of 96 individual optimizations, took 4 minutes and 17 seconds in total to compute, while the longest individual optimization took 10 seconds. Computation times do not change if initialization parameters, starting number of vehicles $n^{\text{bat}}_{0,n}$ and deliveries $N^{\text{out}}_{t,k,n}$, are scaled up.

The presented models successfully exploit the matrix sparsity. This is particularly important for variable $x^{\text{out}}_{t,k,n,m}$, which in its dense form has slightly over 4 million combinations (96 x 96 x 21 x 21), but in the sparse form for the presented case study there are only 2,318 combinations sent to the solver. To further improve the implementation, we also implement sparsity on the auxiliary charging matrix as represented by the shaded elements in Fig. 1. Such large number of variables would force a solver to spend much time in the presolve and basically render the model unscalable for larger problem

TABLE VII
SHARE OF RELAXED VARIABLES WITH INTEGER VALUES (IN [%])

Γ	$n^{\text{bat}}_{t,n}$ (2016 vars)	$n^{\text{aux}}_{t,n,m}$ (17760 vars)	$x^{\text{out}}_{t,k,n,m}$ (2318 vars)	$x^{\text{in}}_{t,n}$ (1632 vars)
0	88.1	98.6	98.4	97.7
8	75.8	97.0	98.8	98.3

instances. Additionally, a dense model cannot even be built in slower modeling languages, e.g. Python Pyomo or YALMIP [34], since even GAMS takes 15 seconds to build it and creates 1.2 GB model file in the process, as opposed to 0.1 seconds and 12 MB for the sparse version.

We compare the computation time of our day-ahead model to the traditional, declusterized approach modeling the same level of details. Taking $\Gamma = 8$ as a computation reference, our model is solved within 7 seconds to 0.1% optimality gap, while the declusterized formulation takes 822 seconds to find a first solution with 0.67% optimality gap. Computational complexity of the declusterized approach grows proportionally with the number of EVs in the fleet and the number of different deliveries, while complexity of the clustered approach is proportional only to the number of different deliveries thus scales well. Two deliveries are different if they vary in at least one of the following parameters: starting time, trip duration, and energy consumed during the trip.

Cluster resolution is decided based on trade-off between computational tractability and desired accuracy. The number of variables in the auxiliary charging matrix grows quadratically with the number of clusters, thus slowing down the computations. However, even 101 cluster resolution (one for each 1% SoE) is still reasonably tractable since it takes 145 seconds to solve the problem for the base case study ($\Gamma = 8$ and 100 EVs) as opposed to 6 seconds when 21 cluster is used. The 21-cluster resolution is used for the case studies as it is deemed sufficient to capture battery nonlinearities and relevant operations for the station, while also leaving more than enough computational resources for scaling the model to larger or more complicated instances.

While the presented case study was solved using the solver's default settings, internal testings show that the solver's relaxed root LP computation takes increasingly longer to compute when simulating longer time periods, e.g. a week or a month, or when increasing the number of clusters. However, this is easily solved by setting the solver to run using the barrier algorithm for root LP (option *method=2*), which is known to better scale for large problems and outperform the default simplex algorithm [35]. To verify this, we report that the computation time for scheduling the charging station over a period of one week using 15-minute intervals was less than 15 seconds for the barrier algorithm, while the simplex algorithm took up to 3 minutes.

VI. CONCLUSION

This paper models the operation of a charging station for EV delivery fleet featuring more details than a single aggregate battery approach found in the literature and scales better than modelling individual EVs. The model can be used to reduce the charging station's expenses by deciding when and how much to charge specific vehicles. It also demonstrates that the common assumption that EVs should always leave the station fully charged is far from optimal. In the presented case study, such policy required 26% more EVs to fulfill all the deliveries and had 3% higher charging costs as compared to the proposed model.

Despite the optimistic battery parameters used in the case study (battery cost 300 €/kWh and 5,000 cycles during lifetime), no energy is sold in the market. This is a direct consequence of low price spread imposed by the robust subproblem and very dense delivery schedule that does not leave much battery capacity for performing arbitrage. However, if more battery capacity would be available for arbitrage, the EVs would perform one cycle with the given market prices.

The presented analysis on the effect the number of chargers has on the objective function can be a valuable investment tool that determines the optimal power capacity and number of chargers at the station. On the other hand, the analysis of the battery size and degradation effects on the objective function can help potential investors find an optimal battery capacity to reduce electricity costs by performing an adequate level of arbitrage.

High tractability of the presented approach allows for implementation of intraday MPC strategy. The results show that MPC achieves objective function within 5.5% of the case when perfect information are used. It also guarantees operation feasibility since it assumes the worst-case trip realizations.

REFERENCES

[1] K. Davis, P. Rowley and S. Carroll, "Assessing the viability of electric vehicle technologies for UK fleet operators," *48th International Universities' Power Engineering Conference (UPEC)*, pp. 1–6, Dublin, Sept. 2013.

[2] A. Ottensmann, J. Haubrock and D. Westermann, "Forecast of the aggregated charging power of electric vehicles in commercial fleets," *2014 IEEE International Electric Vehicle Conference (IEVC)*, pp. 1–5, Florence, Dec. 2014.

[3] X. Gan *et al.*, "Fast-Charging Station Deployment Considering Elastic Demand," *IEEE Transactions on Transportation Electrification*, vol. 6, no. 1, pp. 158–169, March 2020.

[4] M. A. Ortega-Vazquez, "Optimal scheduling of electric vehicle charging and vehicle-to-grid services at household level including battery degradation and price uncertainty," *IET Generation, Transmission & Distribution*, vol. 8, no. 6, pp. 1007–1016, June 2014.

[5] H. Pandžić and V. Bobanac, "An Accurate Charging Model of Battery Energy Storage," *IEEE Transactions on Power Systems*, vol. 34, pp. 1416–1426, March 2019.

[6] M. Ecker *et al.*, "Calendar and cycle life study of Li(NiMnCo)O2-based 18650 lithium-ion batteries," *Journal of Power Sources*, vol. 248, pp. 839–851, Feb. 2014.

[7] CanadianSolar, "Three phase string inverter 50-66 KW" [Online] Available at: tinyurl.com/yy7zmvyo

[8] O. Sundstrom and C. Binding, "Optimization Methods to Plan the Charging of Electric Vehicle Fleets," *Proceedings of International Conference on Control, Communication and Power Engineering (CCPE)*, pp. 323–328, Chennai, India, July 2010.

[9] T. Lan, J. Hu, Q. Kang, C. Si, L. Wang and Q. Wu, "Optimal control of an electric vehicle's charging schedule under electricity markets," *Neural Computing and Applications*, vol. 23, pp. 1865–1872, Dec. 2013.

[10] J. Xu and V. W. S. Wong, "An approximate dynamic programming approach for coordinated charging control at vehicle-to-grid aggregator," *IEEE International Conference on Smart Grid Communications*, pp. 279–284, Brussels, Oct. 2011.

[11] S. I. Vagropoulos, D. K. Kyriazidis, and A. G. Bakirtzis, "Real-Time Charging Management Framework for Electric Vehicle Aggregators in a Market Environment," *IEEE Transactions on Smart Grid*, vol. 7, no. 2, pp. 948–957, March 2016.

[12] R. Moghaddass, O. A. Mohammed, E. Skordilis, and S. Asfour, "Smart Control of Fleets of Electric Vehicles in Smart and Connected Communities," *IEEE Transactions on Smart Grid*, vol. 10, no. 6, pp. 6883–6897, Nov. 2019.

[13] S. Vandael, B. Claessens, D. Ernst, T. Holvoet, and G. Deconinck, "Reinforcement Learning of Heuristic EV Fleet Charging in a Day-Ahead Electricity Market," *IEEE Transactions on Smart Grid*, vol. 6, no. 4, pp. 1795–1805, July 2015.

[14] O. Sassi and A. Oulamara, "Electric Vehicle Scheduling and Optimal Charging Problem: Complexity, Exact and Heuristic Approaches," *International Journal of Production Research*, vol. 55, pp. 519–535, June 2016.

[15] H. Zhang, Z. Hu, Z. Xu, and Y. Song, "Evaluation of Achievable Vehicle-to-Grid Capacity Using Aggregate PEV Model," *IEEE Transactions on Power Systems*, vol. 32, no. 1, pp. 784–794, Jan. 2017.

[16] B. Škugor and J. Deur, "A novel model of electric vehicle fleet aggregate battery for energy planning studies," *Energy*, vol. 92, pp. 444–455, Dec. 2015.

[17] K. Šepetanc and H. Pandžić, "A Cluster-based Operation Model of Aggregated Battery Swapping Stations," *IEEE Transactions on Power Systems*, vol. 35, no. 1, pp. 249–260, Jan. 2020.

[18] M. Wang *et al.*, "State Space Model of Aggregated Electric Vehicles for Frequency Regulation," *IEEE Transactions on Smart Grid*, vol. 11, no. 2, pp. 981–994, March 2020.

[19] M. Alizadeh *et al.*, "Reduced-Order Load Models for Large Populations of Flexible Appliances," *IEEE Transactions on Power Systems*, vol. 30, no. 4, pp. 981–994, July 2015.

[20] J. M. Foster and M. C. Caramanis, "Optimal Power Market Participation of Plug-In Electric Vehicles Pooled by Distribution Feeder," *IEEE Transactions on Power Systems*, vol. 28, no. 3, pp. 2065–2076, Aug. 2013.

[21] M. Alizadeh, G. Kesidis and A. Scaglione, "Clustering consumption in queues: A scalable model for electric vehicle scheduling," *Asilomar Conference on Signals, Systems and Computers*, Pacific Grove, CA, 2013, pp. 374-378.

[22] S. Bashash and H. K. Fathy, "Transport-Based Load Modeling and Sliding Mode Control of Plug-In Electric Vehicles for Robust Renewable Power Tracking," *IEEE Transactions on Smart Grid*, vol. 3, no. 1, pp. 526–534, March 2012.

[23] S. I. Vagropoulos and A. G. Bakirtzis, "Optimal Bidding Strategy for Electric Vehicle Aggregators in Electricity Markets," *IEEE Transactions on Power Systems*, vol. 28, no. 4, pp. 4031–4041, Nov. 2013.

[24] A. Sakti *et al.*, "Enhanced representations of lithium-ion batteries in power systems models and their effect on the valuation of energy arbitrage applications," *Journal of Power Sources*, vol. 342, pp. 279–291, Feb. 2017.

[25] C. Diaz, A. Mazza, F. Ruiz, D. Patino and G. Chicco, "Understanding Model Predictive Control for Electric Vehicle Charging Dispatch," *2018 53rd International Universities Power Engineering Conference (UPEC)*, Glasgow, 2018, pp. 1–6.

[26] Y. Shi, H. D. Tuan, A. V. Savkin, T. Q. Duong and H. V. Poor, "Model Predictive Control for Smart Grids With Multiple Electric-Vehicle Charging Stations," *IEEE Transactions on Smart Grid*, vol. 10, no. 2, pp. 2127–2136, March 2019

[27] C. Diaz, F. Ruiz and D. Patino, "Smart Charge of an Electric Vehicles Station: A Model Predictive Control Approach," *2018 IEEE Conference on Control Technology and Applications (CCTA)*, Copenhagen, 2018, pp. 54–59.

[28] Y. Zheng, Y. Song, D. J. Hill and K. Meng, "Online Distributed MPC-Based Optimal Scheduling for EV Charging Stations in Distribution Systems," *IEEE Transactions on Industrial Informatics*, vol. 15, no. 2, pp. 638–649, Feb. 2019.

[29] D. Bertsimas and M. Sim, "The Price of Robustness," Aug. 2001. [Online] Available at: robustopt.com/references/Price%20of%20Robustness.pdf

[30] B. Škugor and J. Deur, "Delivery vehicle fleet data collection, analysis and naturalistic driving cycles synthesis," *International Journal of Innovation and Sustainable Development*, vol. 10, pp. 19–39, Jan. 2016.

[31] NREL, "Cost Projections for Utility-Scale Battery Storage," June 2019. [Online] Available at: nrel.gov/docs/fy19osti/73222.pdf

[32] Nord Pool, "Elspot Prices_2018_Hourly_EUR," Jan. 2019. [Online] Available at: nordpoolgroup.com/globalassets/marketdata-excel-files/elspot-prices_2018_hourly_eur.xls

[33] GAMS Code for the Cluster-Based Model for Charging a Fleet of Electric Vehicles. [Online] Available at: github.com/KSepetanc/EV-Delivery-Station

[34] I. Dunning, J. Huchette and M. Lubin, "JuMP: A modeling language for mathematical optimization," *SIAM Review*, vol. 59, no. 2, pp. 295–320, May 2017.

[35] Gurobi 8.1 Documentation, Choosing the right algorithm. [Online] Available at: gurobi.com/documentation/8.1/refman/numerics_choosing_the_righ.html